A polylactide/fibrin gel composite scaffold for cartilage tissue engineering: fabrication and an in vitro evaluation

Haiguang Zhao · Lie Ma · Yihong Gong ·
Changyou Gao · Jiacong Shen

Abstract A composite scaffold for cartilage tissue engineering was fabricated by filling a porous poly (L-lactide) (PLLA) scaffold with fibrin gel. The porous PLLA scaffold prepared by a method of thermally induced phase separation has an average pore diameter of 200 μm and a porosity of 93%. Incorporation of fibrin gel into the scaffold was achieved by dropping a fibrinogen and thrombin mixture solution onto the scaffold. For a couple of minutes the fibrin gel was in situ formed within the scaffold. The filling efficiency was decreased along with the increase of the fibrinogen concentration. After fibrin gel filling, the compressive modulus and the yield stress increased from 5.94 MPa and 0.37 MPa (control PLLA scaffold in a hydrated state) to 7.21 MPa and 0.53 MPa, respectively. While the fibrin gel lost its weight in phosphate buffered saline up to ∼50% within 3 days, 85% and 70% of the fibrin gel weight in the composite scaffold was remained within 3 and 35 days, respectively. A consistent significant higher level of rabbit auricular chondrocyte viability, cell number and glycosaminoglycan was measured in the composite scaffold than that in the control PLLA scaffold. Rabbit auricular chondrocytes with round morphology were also observed in the composite scaffold by confocal microscopy and scanning electron microscopy. Altogether with the features of better strength and cytocompatibility, this type of composite scaffold may have better performance as a matrix for cartilage tissue engineering.

1 Introduction

Tissue engineering and regenerative medicine has emerged as a new approach in treatment of damaged or disabled tissues/organs such as bone, cartilage and skin [1]. Many kinds of porous scaffolds have been fabricated using different biomaterials and by various methods in order to provide physical support. However, natural extra-cellular matrix (ECM) does not only take a role of simple physical support for the cells. It provides a substrate containing adhesion proteins for cell adhesion, proliferation and differentiation. Therefore, artificial ECM has been studied carefully in many previous works in order to mimic both the chemical compositions and the physical structures [2–5].

Two types of physical structures have been utilized as the scaffolds: porous scaffolds and hydrogels. The porous scaffolds are usually made from synthetic biodegradable polymers such as polylactide (PLA), poly (glycol acid) (PGA) and their copolymers (PLGA) as well as polycaprolactone (PCL). They have good mechanical strength and shape-persistency during both in vitro and in vivo cultures. Several techniques such as porogen leaching [6], phase separation [7, 8], fiber processing [9], and 3D micro-printing [10] have been used to produce porous scaffolds with variable microstructures. However, this kind of materials is unlikely to induce cell adhesion and tissue regeneration. Most cells tend to adhere and spread only on the scaffold surfaces. Therefore, the morphology and distribution of cells are quite different from those in their natural state, for example chondrocytes in natural cartilage matrix [11, 12].

H. Zhao · L. Ma (✉) · Y. Gong · C. Gao (✉) · J. Shen
Key Laboratory of Macromolecular Synthesis and
Functionalization, Ministry of Education, Department
of Polymer Science and Engineering, Zhejiang University,
Hangzhou 310027, China
e-mail: liema@zju.edu.cn

C. Gao
e-mail: cygao@zju.edu.cn; cygao@mail.hz.zj.cn

By contrast, naturally originated biopolymers such as collagen, chitosan, proteoglycans and noncollagenous proteins can be highly hydrated, providing a good environment for the cells to proliferate and differentiate [13–17]. These polymers are frequently used in a format of hydrogel, a softer structure with much lower mechanical strength than that of the porous scaffold. Among the hydrogels used so far, fibrin gel is more attractive since it can be obtained autologously and has good biocompatibility. This is of great advantage to avoid the potential risks of foreign body reaction and virus infection. Moreover, the fibrin gel is easily formed by a reaction between fibrinogen and thrombin with the effect of Factor XIIIa [18–22]. Previous results indeed show that cells entrapped in the fibrin gels can produce more collagen [23, 24] and elastin [25]. However, besides the lower mechanical strength, the naturally originated polymers such as the fibrin gel are usually degraded too fast in comparison with the tissue growth rate, such as cartilage [26, 27].

It is known that cartilage damage occurs frequently owing to sports and progressive ageing. Cartilage defect cannot be spontaneously repaired. This limited self-repair capacity of the cartilage forced researchers to develop new technologies and suitable biomaterials to promote tissue integration. In recent years, cartilage regeneration has achieved great success by method of tissue engineering and regenerative medicine. Although the fibrin gel can improve the proliferation and migration of chondrocytes [28, 29], its mechanical strength is generally low, especially for high-loaded cartilage tissue. Optimization of the gelation parameters [30] or compounding with PGA fibers [31] can improve the mechanical performance more or less. In this work, another strategy of compounding is applied to obtain a PLLA/fibrin gel composite scaffold. The soft fibrin gel (instead of the agar hydrogel [32]) is filled into the pores of the PLLA scaffold, resulting in a scaffold having both good biocompatibility and mechanical performance. Moreover, this simple strategy can avoid the tedious surface modification of PLLA scaffold as well, which is often required for the purpose of improvement of cell compatibility. Unlike the agar which is non degradable, the fibrin gel is readily absorbable, making the composite more applicable in practice. In vitro cell culture is performed to assess the efficacy of the composite scaffold on chondrocyte proliferation and ECM production.

2 Materials and methods

2.1 Materials

PLLA (Mn = 200 kDa, Mw = 400 kDa) was purchased from China Textile Academy [33]. Fresh frozen human plasma was kindly donated by Blood Center of Zhejiang Province. Fibrinogen was prepared by a freeze–thaw circling method described previously [34, 35]. Thrombin (400 U) and aprotinin (630 U/mg) were purchased from Sigma-Aldrich and Roche, respectively. All the other chemicals were used as received. Triple-distilled water was used throughout the experiments.

2.2 Preparation of PLLA porous scaffold

The PLLA porous scaffold was fabricated by thermally induced phase separation (TIPS) [7]. Briefly, 5% PLLA/1,4-dioxane–H_2O (87:13, V:V) solution in a glass mold (12 mm diameter and 15 mm in height) at 70°C was quickly quenched to 25°C, followed by coarsening at 25°C for 5 h. The solvent was then solidified at –20°C for 2 h, and was removed by freeze-drying. The PLLA scaffold with an average pore diameter of ~ 200 μm and a porosity of 93% was obtained. The inner microstructure of the PLLA scaffold was observed under scanning electron microscopy (SEM, JEOL JEM). Macroscopic image of the PLLA scaffold was taken by a digital camera.

2.3 Clotting time of the fibrin gel

After mixing the solutions of fibrinogen and thrombin, turbidity change of the mixture solution was monitored immediately by a UV–Vis spectrophotometer (UV-2550, SHIMADZU). The clotting time is defined as the time at which the maximum value appears in the differentiation curve. Each value was averaged from three parallel experiments.

2.4 Preparation of the PLLA/fibrin gel composite scaffold

PLLA/fibrin gel composite scaffold was fabricated by loading the fibrin gel into the wet PLLA scaffold. Firstly, the PLLA scaffold (3 mm in height) was immersed into an alcohol solution (75%) for 1 h, followed by displacing the alcohol with phosphate buffer saline (PBS, pH 7.4) for 2 h. The fibrinogen solution (40 mg/ml) was mixed with a same volume of thrombin with a concentration of 10 U/ml in 40 mM $CaCl_2$ solution. The mixture solution was immediately dropped onto the surface of the wet PLLA scaffold, which was spontaneously absorbed into the scaffold by gravity force and capillary force. The composite scaffold was then incubated at 37°C for 15 min to mature the fibrin gel. To observe distribution of the fibrin gel in the PLLA scaffold, fibrinogen solution was initially mixed with 1 mg/ml fluorescein sodium solution. Fluorescent image was then taken by confocal laser scanning microscopy (CLSM, Bio-Rad Radiance 2100).

Incorporation ratio (R) of the fibrin gel is defined as $((W_m - W_0)\rho/c))/W_c \times 100\% = ((W_m - W_0)\rho/c)/(porosity \times$

$(W_0/\rho_{PLLA}/ (1 - \text{porosity})) \times 100\%)$, where W_0 and W_m are weights of the PLLA scaffold and of the dried PLLA/fibrin gel composite scaffold, respectively, c and ρ are the final concentration and density of the fibrin gel, respectively. The ρ_{PLLA} of PLLA and the porosity of the PLLA scaffold are 1.27 g/cm^3 and 93%, respectively. Each value was averaged from five parallel experiments.

2.5 Weight retention

Weight retention of the scaffold incubated in PBS (pH 7.4) was gravimetrically monitored. Briefly, the PLLA/fibrin gel composite scaffolds and the fibrin gel control were incubated in 3 ml PBS at 37°C. PBS was changed every 2 days. Amount of the degraded or released proteins in the supernatant was measured by UV–Vis spectroscopy (UV-2550, SHIMADZU) at 278 nm. The optical density was referred to a calibration curve recorded from fibrinogen at the same wavelength. The weight retention of the fibrin gel is defined as the percentage of the remaining weight to the initial weight. Each value was averaged from five parallel experiments.

2.6 Mechanical property

The composite scaffolds with a cylindrical shape, i.e. $\sim$10 mm in diameter and $\sim$12 mm in height, were compressed by a mechanical tester (ZWICK ROELL, Germany). The PLLA scaffold without fibrin gel was chosen as a control. The cross-head speed was set at 1 mm/min. The compressive modulus was determined from the compressive curve at the initial strain of 2–6%. Yield stress was defined as the stress at which the strain is leveled off or decreased. Each value was averaged from 3 parallel experiments.

2.7 Cell culture test

Chondrocytes were isolated from cartilage tissue of rabbit ears (New Zealand Rabbit) under the institutional guideline and routinely cultured [36]. Briefly, chondrocytes were isolated by incubating the cartilage pieces in Dulbecco's minimum essential medium (DMEM) containing 0.2% collagenase type II (Sigma) at 37°C for 4–6 h under agitation. The isolated chondrocytes were then centrifuged and resuspended in DMEM supplemented with 10% fetal calf serum (FBS), 300 mg/l glutamine, 50 mg/l vitamin C, 100 U/ml penicillin and streptomycin. The chondrocyte suspension was then seeded in 11 cm tissue culture dishes (Falcon, seeding density 2×10^4 cells/cm^2) and incubated in a humidified atmosphere of 95% air, 5% CO$_2$ at 37°C. Chondrocytes were harvested using 0.25% trypsin when a confluent cell layer was formed (about 3–4 days).

Before cell seeding, the PLLA scaffold ($\sim$5 mm in diameter and $\sim$1 mm in height) was sterilized by 75% ethanol for 2 h and washed by PBS for several times, and then incubated in PBS for 1 day to displace the remaining ethanol. The chondrocyte suspension was mixed with equal volume of thrombin (10 U/ml, 40 mM CaCl$_2$ solution and 2×10^6 cells) and fibrinogen (40 mg/ml, 0.9% NaCl solution) containing 50 U/ml aprotinin. Then the mixed solution was incorporated into the scaffold, and was incubated at 37°C for 10 min to form fibrin gel. As a control, the chondrocyte suspension with the same density was directly injected into the porous PLLA scaffold from both sides. Finally, both of the cell-seeded PLLA /fibrin gel composite scaffold and the porous PLLA scaffold were cultured in the complete medium statically. To observe cell distribution under CLSM, the cell-containing scaffold was taken out from the culture plate and rinsed with PBS gently. Then 1 mg/ml fluorescein diacetate (FDA)/PBS solution was slowly injected into the scaffold. After incubated for 10 min the scaffold was gently cut into several parts. By this fluorescently staining, only the viable cells in the scaffold can be visualized under CLSM. To observe the morphology of the chondrocytes, the samples were fixed with 2.5% glutaraldehyde solution at 4°C for 12 h and dehydrated with a graded series of ethanol. Then the scaffolds were further dehydrated with acetone and treated with isoamyl acetate, each for 15 min. After being dried by a critical point dry method, the scaffold was coated with an ultrathin gold layer and observed under scanning electron microscopy (SEM, Cambridge stereoscan 260).

Cell viability in the composite scaffold was measured by a methylthiazoletetrazolium (MTT) method. 100 µl MTT solutions (5 mg/ml) was added into each well (24 well culture dishes) and cultured for 4 h. After adding 1 ml dimethyl sulphoxide, the mixture was centrifuged at 10,000 rmp for 10 min to ensure a complete separation of formazan pigment from the scaffold. Absorbance at 570 nm was measured on a microplate reader (Bio-Rad 550). Each value was averaged from three parallel experiments.

The cell amount in the scaffold was assessed by quantifying DNA using Hoechst 33258 (Sigma) assay [37]. Hoechst 33258 is a bis-benzimide derivative that can bind to the AT-rich regions of double stranded DNA and is excited in near UV (360 nm) and emits in the blue region (450 nm). The sample was frozen at −20°C for 1 h, lyophilized for 2 h for 3 times, and digested with 300 µl 1% w/v papain/0.09% disodium ethylenediaminetetraacetic acid (EDTA) solution [38]. Shortly after digestion, 2 ml Hoechst 33258 solution (1 µg/ml) was added. Then the fluorescence intensity at 450 nm was recorded by a fluorescent spectrophotometer (RF-5301PC, Shimadzu). The cell number was obtained by referring to a calibration curve recorded from known number of cells at the same wavelength. Each value was averaged from three parallel experiments.

To measure the sulphated glycosaminoglycan (GAG) content, 1, 9-dimethylmethylene blue assay was employed

[39]. Briefly, the sample was cut into small pieces and digested with papain buffer solution (5 g/l papain, 0.1 M KH_2PO_4, 5 mM EDTA and 5 mM cysteine · HCl, pH 6.0) at 60°C for 6 h. The dye solution prepared by dissolving 16 mg of 1,9-dimethylmethylene blue in 1 l distilled water containing 3.04 g glycine, 2.37 g NaCl and 95 ml 0.1 M HCl was then added into the mixture. After 5 min, absorbance at 525 nm was measured by UV–Vis spectroscopy. The content of GAG secreted by the chondrocytes in the scaffold was determined by referring to a calibration curve of chondroitin sulfate. Data were presented as GAG amount per scaffold volume (in vitro). Each value was averaged from three parallel experiments.

2.8 Statistical analysis

Data are expressed as mean ± standard deviation (SD). Statistical analysis was performed using two-population Student's *t*-test. The significant level was set as $P < 0.05$.

3 Results and discussion

3.1 Macro-and micro-structures of the PLLA/fibrin gel scaffold

A recent study by our group showed that there is no significant difference between the scaffolds with a pore size of 150 μm and 350 μm in terms of the hydrogel loading. However, the PLLA scaffold with a smaller pore size has a stronger mechanical property compared to that with a larger pore size [7]. Therefore, in this work the porous PLLA scaffold with an average pore size of 200 μm and a porosity of 93% was used to obtain the composite scaffold. Figure 1 shows the macroscopic shape (Fig. 1a) and microscopic structure (Fig. 1b) of the scaffold. The macroscopic shape was controlled by the mold and is readily tailored by post mechanical manufacture. The microscopic structure was customized by the phase separation conditions such as solvent quality, quenching rate and coarsening time [7]. Here the coarsening time strategy was applied to obtain the scaffold with good pore interconnectivity as shown in Fig. 1b, which is further evidenced by the infiltration of the fibrin gel (Fig. 1d). It shows that the fibrin gel (green regions) distributed evenly through the pores of the PLLA scaffold. Macroscopic appearance of the pure fibrin gel is shown in Fig. 1c for comparison.

3.2 Factors controlling incorporation of the fibrin gel

Even distribution and sufficient infiltration of the fibrin gel favors the subsequent cell loading and construction of a homogeneous tissue. It is known that the fibrin gel is formed by mixing the solutions of fibrinogen and thrombin [18–22], whose clotting time can be controlled ranging from several seconds to several minutes by altering the

Fig. 1 Macroscopic images of (**a**) PLLA porous scaffold and (**c**) fibrin gel (FG). The microstructures of PLLA porous scaffold and fibrin gel incorporated scaffold are observed by (**b**) SEM and (**d**) CLSM, respectively
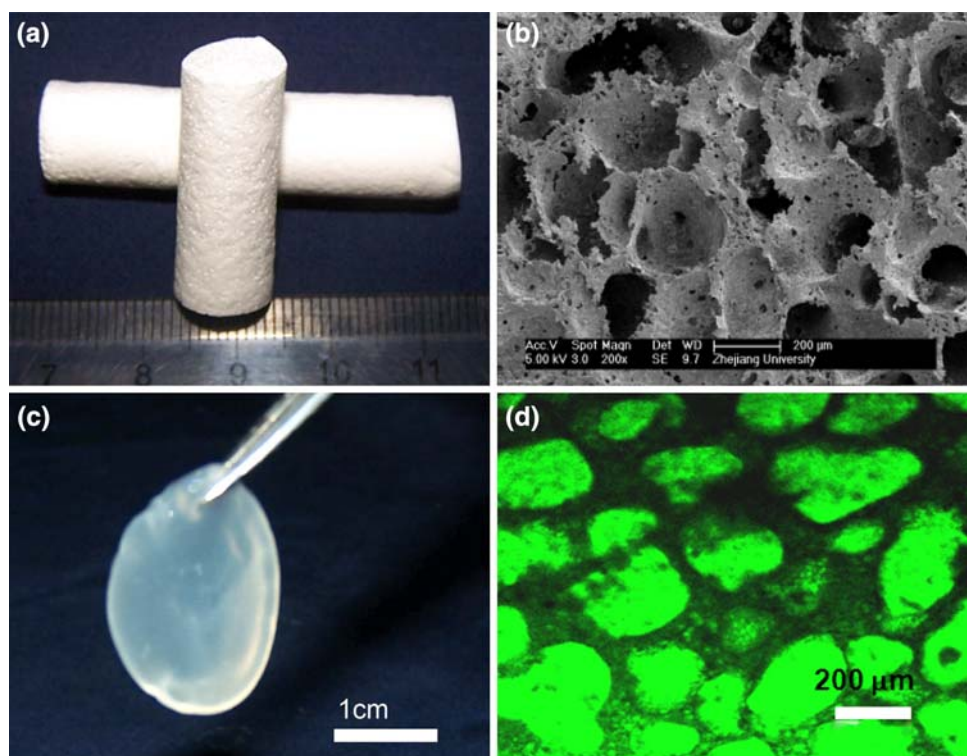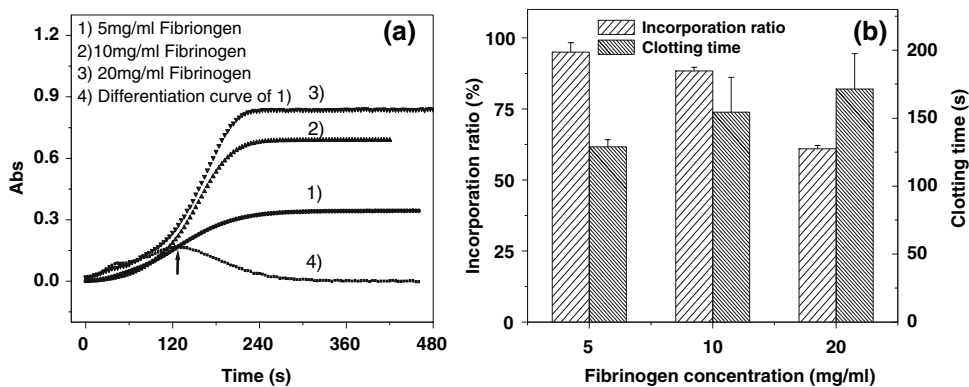
Fig. 2 (**a**) Absorbance of fibrin gel at 550 nm as a function of reaction time. Arrow in curve (4) indicates the maximum change time. (**b**) The incorporating ratio and clotting time of the fibrinogen as a function of fibrinogen concentration. The clotting time is defined as

the time at which the maximum change occurs in the differentiation curve as shown in (**a**). The thrombin concentration was kept constant at 5 U/ml

concentration of thrombin [18–22, 35]. In order to load the fibrin gel into the PLLA scaffold with a higher ratio, the system with a longer clotting time was thus adopted. After clotting at room temperature for several minutes, the transparent mixture solution will lose its fluidity and is transformed into an opaque hydrogel as shown in Fig. 1c. During this process, the clotting time and hydrogel concentration are the main factors influencing the loading efficiency of the overall fibrin gel. We found that clotting of the fibrin gel is too fast to handle when the thrombin concentration is larger than 5 U/ml. Therefore, the thrombin concentration was set as 5 U/ml in the present study.

The clotting process of the fibrin gel was monitored by UV–Vis spectroscopy. Figure 2a shows that absorbance of the fibrin gel at 550 nm increased along with the time prolongation for all the samples. The corresponding clotting time as a function of the fibrinogen concentration is displayed in Fig. 2b. Along with the increase of the fibrinogen concentration, the clotting time was slightly increased from 123 s (5 mg/ml fibrinogen) to 164 s (20 mg/ml fibrinogen) at 25°C. This period is long enough to load the fibrin gel into the PLLA scaffold. The incorporating ratio of the fibrin gel was decreased rapidly from 95% (5 mg/ml fibrinogen) to 62% (20 mg/ml fibrinogen) along with the increase of the

fibrinogen concentration. This is attributed to the viscosity increase, which makes the spontaneous loading by gravity force and capillary force become more difficult.

3.3 Mechanical property of the composite scaffold

In cartilage tissue engineering, the implanted scaffolds should maintain their designed macro- and micro-structures during the healing period and must be mechanically strong to bear the load. Therefore, mechanical property of the scaffolds plays an important role in the cartilage regeneration. Some composite scaffolds comprising biomacromolecules such as alginate and collagen and polymer meshes have been utilized in tissue engineering and shown good cytocompatibility [40, 41]. Furthermore, PLLA offers an important combination of mechanical stability and retention of cellular phenotype, in particular improved proteoglycan production by chondrocytes over other polymer scaffolds as demonstrated by Rahman and Tsuchiya [42]. In our strategy, a PLLA scaffold with a porous microstructure was used instead of polymer meshes, providing much stronger mechanical strength [32]. Figure 3a shows the stress–strain curves of the PLLA scaffolds with or without incorporation of fibrin gel. When the strain was lower than 10%, the stress

Fig. 3 (**a**) Stress–strain curves of a PLLA porous scaffold with an average pore diameter of 200 μm in a wet state and a FG incorporated scaffold; (**b**) the compressive modulus and yield stress derived from the curves in (**a**). The fibrin gel in both cases was obtained from 20 mg/ml fibrinogen and 5 U/ml thrombin
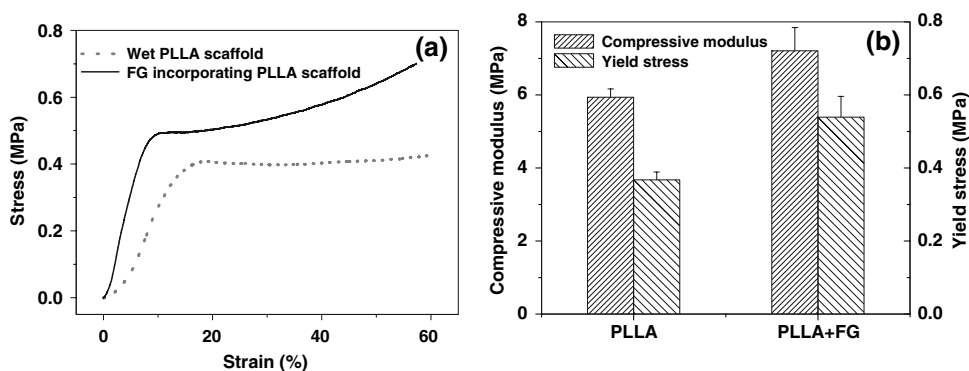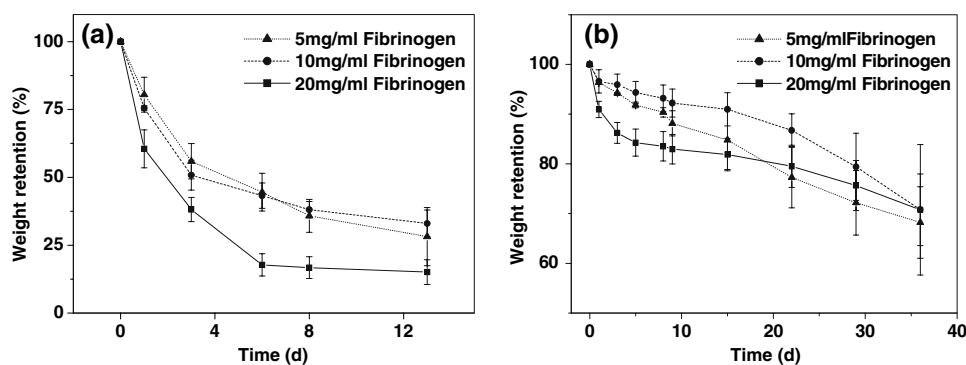
Fig. 4 Weight retention of (**a**) fibrin gel and (**b**) FG incorporated scaffold with different fibrinogen concentration. All samples were fabricated with 5 U/ml thrombin and 25 U/ml aprotinin

increased almost linearly. Platform regions appeared when the strains exceeded 15–20%. In the linearly increased region from 2% to 6%, the deformation extent was small and can be regarded as elastic. Therefore, the compressive modulus could be calculated (Fig. 3b). A higher compressive modulus (7.21 MPa) for the composite scaffold was found than that of the control PLLA scaffold in a hydrated state (5.94 MPa). Figure 3b also shows that the yield stress of the composite scaffold (0.53 MPa) was higher than that of the control PLLA scaffold (0.37 MPa). The higher modulus and yield stress of the composite scaffold is certainly attributed to the reinforcement effect of the filled fibrin gel. This is beneficial to constructing cartilage in a tissue engineering way. The composite scaffold provides a more rigid and consistent mechanical structure for the tissue-engineered constructs, and therefore has significant advantages in terms of mechanical performance and surgical-handling property.

3.4 Weight retention of the composite scaffold

Weight retention of the fibrin gel and the composite scaffolds in PBS was monitored as a function of the incubation time (Fig. 4). As shown in Fig. 4a, all kinds of the fibrin gels, regardless of the fibrinogen concentration, lost their weights very quickly during the first 3 days, at which only ∼50% of the initial weight was preserved. Commercially available fibrin glues have lower mechanical strength, and tend to disintegrate in vitro and in vivo after several days and almost completely dissolve within 3–4 weeks [30, 43]. Together with our previous results [35], the weight loss is thus more likely caused by dissolution rather than degradation of the fibrin gel. In contrast, the speed of weight loss of the fibrin gel was significantly delayed in the composite scaffolds (Fig. 4b). At day 3, more than 85% of the fibrin gel was preserved. Till to day 35, the fibrin gel weight of all the samples was preserved up to 70%. These results indicate that release of the fibrinogen has been significantly retarded. It is reasonable since the fibrin gel loaded in the PLLA scaffold is difficult to escape from the porous structure. Another point in Fig. 4 is that the fibrin gel made from a higher fibrinogen concentration lost its weight more

rapidly than those made from lower concentrations. This is consistent with the above discussion, in which a larger concentration difference between the hydrogel and the bulk PBS creates a larger chemical potential, which drives the release of the solute, namely the fibrinogen.

3.5 Cell culture in vitro

Low seeding efficiency is always a crucial problem for a construct of cells/porous scaffold. By incorporation of the fibrin gel into the porous scaffold, the cell can be easily loaded and maintained in the scaffold with a higher efficiency. As demonstrated by Elvira Malicev and coworkers [44], encapsulation of cells in fibrin gel in the form of human blood plasma or commercially available fibrin glue improves the yield of cell adhesion and results in a more homogenous distribution of cells over the porous collagen scaffold. Furthermore, the highly hydrated fibrin gel can provide a better environment for chondrocyte proliferation and differentiation.

CLSM imaging confirmed that the chondrocytes (green color) were observed in both the control PLLA scaffold (Fig. 5a and b) and the composite scaffold (Fig. 5c and d) after cultured for 7 days in vitro. However, there were a relatively larger number of chondrocytes in the composite scaffold. Meanwhile, the chondrocytes in the composite scaffold distributed more evenly and showed round morphology. In contrast, the cells cultured in the control scaffold showed elongated shape. SEM observation confirmed that in the control scaffold, the cells mostly adhered on the pore walls after 7 days culture (Fig. 6a), and nearly formed monolayers after 14 days culture (Fig. 6b and c). In the composite scaffold, by contrast, most of the chondrocytes were entrapped in the fibrin gel and remained round shape (Fig. 6d, e and f). In native cartilage the chondrocytes show normally round shape and are surrounded by a cross-linked matrix just like the hydrogel. In the present case, the fibrin gel severs as an artificial ECM to embed and support chondrocytes alike their native growth environment. Therefore, the biomimetic structure of the fibrin

Fig. 5 CLSM images to show distribution of chondrocytes seeded in (a) a control PLLA porous scaffold; (c) a PLLA/fibrin gel (20 mg/ml fibrinogen, 5 U/ml thrombin, 25 U/ml aprotinin) scaffold after in vitro cultured for 7 days. (b) and (d) are higher magnification images of (a) and (c), respectively. Cell seeding density was 1×10^6/ml
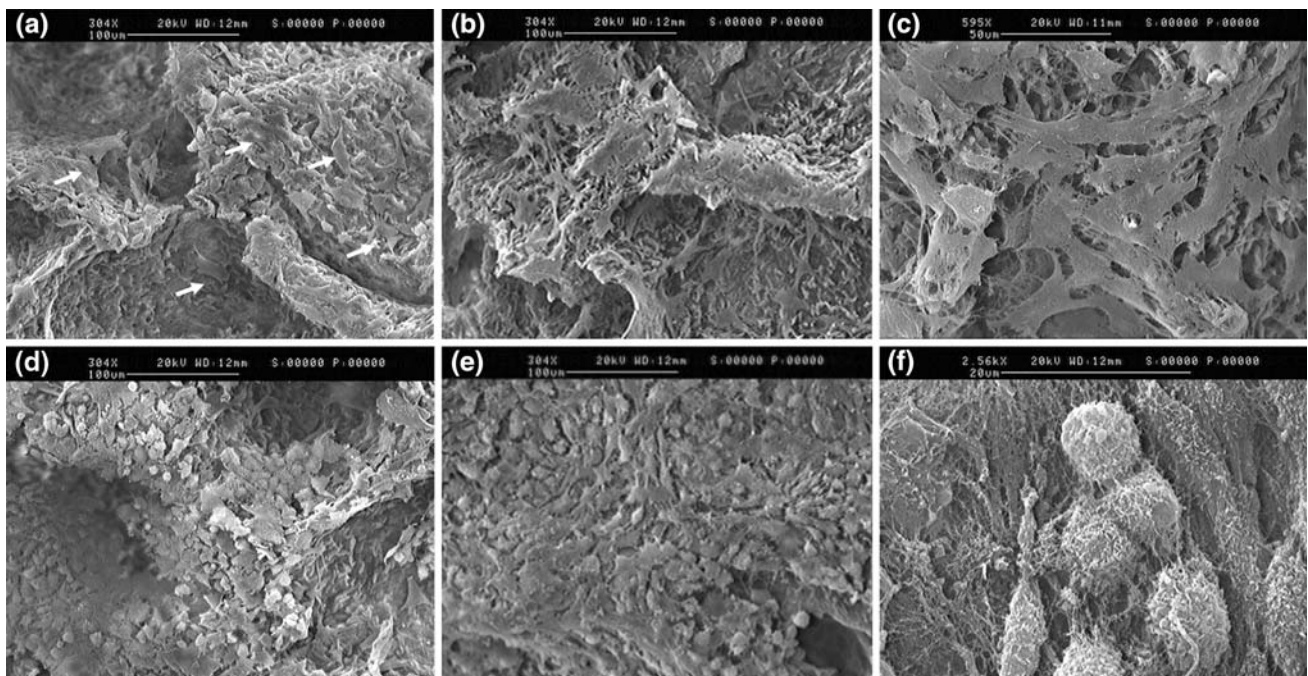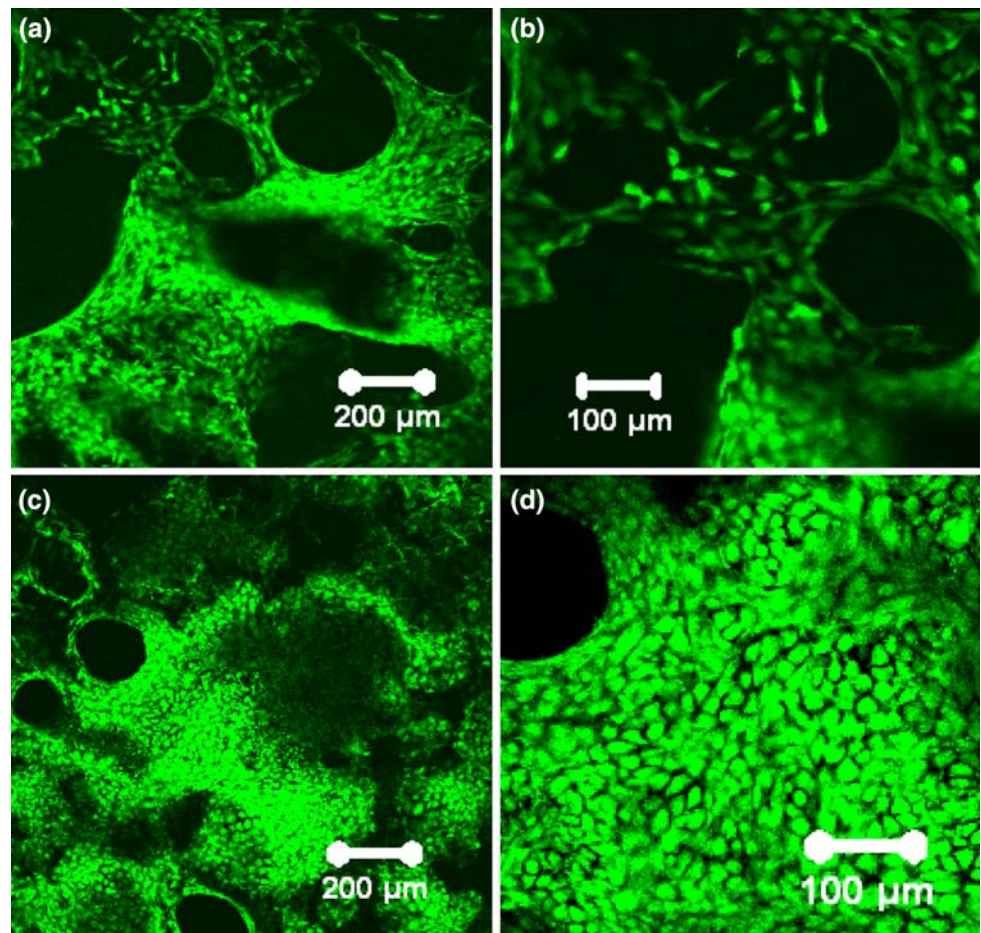

Fig. 6 SEM images to show the chondrocytes seeded in (a, b) a control PLLA scaffold, (d, e) a PLLA/fibrin gel (20 mg/ml fibrinogen, 5 U/ml thrombin, 25 U/ml aprotinin) scaffold. (c) and (f) are higher magnification images of (b) and (d), respectively. The in vitro culture time was 7 days in (a, d), and 14 days in (b, e), respectively. Cell seeding density was 1×10^6/ml

Fig. 7 (**a**) Optical density and (**b**) cell number in the control PLLA scaffold and the PLLA/ fibrin gel (20 mg/ml fibrinogen, 5 U/ml thrombin, 25 U/ml aprotinin) scaffold as a function of culture time in vitro. Cell seeding density was 1×10^6/ml
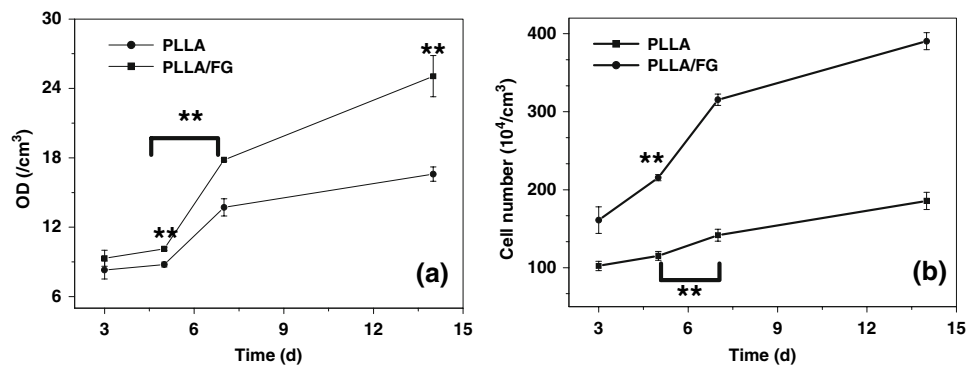
gel-filled scaffold is expected to keep the chondrocytes from dedifferentiation and to increase the cell performance.

The cell proliferation behavior was evaluated by tracing the cell viability and cell number along with the culture time. Figure 7a and b shows that both the cell viability and cell number were increased along with the culture time, especially after day 5, implying that the chondrocytes could normally proliferate. However, compared with the control PLLA scaffold, the composite scaffold has significantly higher value in terms of cell viability and cell number ($P < 0.01$), confirming that the composite environment, originated mostly from the fibrin gel, can promote the proliferation of the chondrocytes in a higher level.

Not only the chondrocytes grow faster, but also they can produce more ECM such as GAGs. Figure 8 compares further the GAG secretion level of the chondrocytes. With the increase of the culture time, the secreted GAG increased in both the composite and the control scaffolds. However, at the same culture intervals, the GAG secretion level in the composite scaffold is always higher than that in the control. Statistical analysis confirms significant

difference ($P < 0.01$) between each time interval. These results demonstrate that the fibrin gel filling strategy can effectively sustain and accelerate the functions of chondrocytes. Further studies are underway to culture the constructs for a longer period and culture in vivo.

4 Conclusions

A composite scaffold is fabricated by incorporating fibrin gel into a PLLA porous scaffold. Incorporation efficiency of the fibrin gel can be controlled by the fibrinogen concentration, which influences the clotting time too. The fibrin gel filling can significantly improve the compressive modulus and yield strength of the scaffold, and slow down the weight loss rate of the fibrin gel. The fibrin gel filling provides also a highly hydrated matrix alike the native ECM of cartilage, resulting in higher cell number and viability and GAG production. Thus, the fibrin gel-filled scaffold is expected to possess better applicability in cartilage tissue engineering.

Fig. 8 The amount of the secreted GAG in the control PLLA scaffold and the PLLA/fibrin gel (20 mg/ml fibrinogen, 5 U/ml thrombin, 25 U/ml aprotinin) scaffold as a function of culture time in vitro. Cell seeding density was 1×10^6/ml

References

1. R. Langer, J.P. Vacanti, Science **260**, 920 (1993). doi:10.1126/science.8493529
2. D.W. Hutmacher, Biomaterials **21**, 2529 (2000). doi:10.1016/S0142-9612(00)00121-6
3. Z.W. Ma, C.Y. Gao, Y.H. Gong, J.C. Shen, J. Biomed. Mater. Res. B **67B**, 610 (2003). doi:10.1002/jbm.b.10049
4. Z.W. Ma, C.Y. Gao, Y.H. Gong, J.C. Shen, Biomaterials **26**, 1253 (2005). doi:10.1016/j.biomaterials.2004.04.031
5. E. Schnell, K. Klinkhamme, S. Balze, G. Brook, D. Klee, P. Dalton et al., Biomaterials **28**, 3012 (2007). doi:10.1016/j.biomaterials.2007.03.009
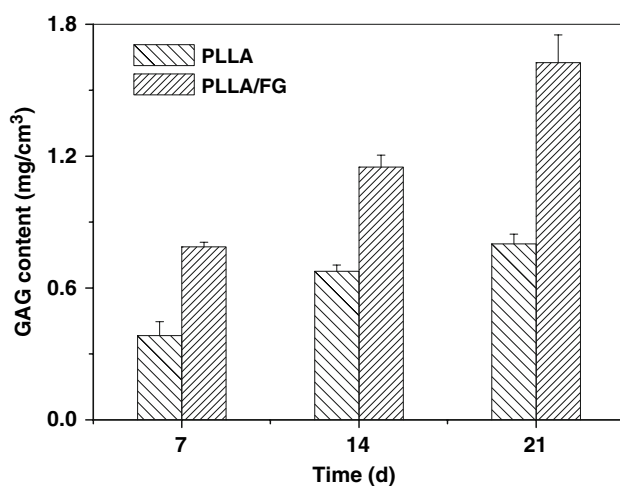6. P.X. Ma, J.W. Choi, Tissue Eng. **7**, 23 (2001). doi:10.1089/107632701300003269

7. Y.H. Gong, Z.W. Ma, C.Y. Gao, W. Wang, J.C. Shen, J. Appl. Polym. Sci. **101**, 3336 (2006). doi:10.1002/app.23931
8. Y.S. Nam, T.G. Park, J. Biomed. Mater. Res. **47**, 8 (1999). doi:10.1002/(SICI)1097-4636(199910)47:1<8::AID-JBM2>3.0. CO;2-L
9. A.G. Mikos, Y. Bao, L. Cima, D.E. Ingber, J.P. Vacanti, R. Langer, J. Biomed. Mater. Res. **27**, 183 (1993). doi:10.1002/jbm.820270207
10. A. Park, B. Wu, L.G. Griffith, J. Biomater. Sci. Polym. Ed. **9**, 89 (1998). doi:10.1163/156856298X00451
11. Y. Deng, K. Zhao, X.F. Zhang, P. Hu, G.Q. Chen, Biomaterials **23**, 404940 (2002). doi:10.1016/S0142-9612(02)00136-9
12. W.J. Li, R. Tuli, R.S. Tuan, Biomaterials **26**, 599 (2005). doi:10.1016/j.biomaterials.2004.03.005
13. J.A. Buckwalter, H.J. Mankin, AAOS. Instr. Course Lect. **47**, 477 (1998)
14. N.P. Cohen, R.J. Foster, V.C. Mow, J. Orthop. Sports Phys. Ther. **28**, 203 (1998)
15. J.S. Temenoff, A.G. Mikos, Biomaterials **21**, 431 (2000). doi:10.1016/S0142-9612(99)00213-6
16. C.W. Archer, P. Francis-West, Int. J. Biochem. Cell Biol. **35**, 401 (2003). doi:10.1016/S1357-2725(02)00301-1
17. B.P. Chan, T.Y. Hui, C.W. Yeung, J. Li, I. Mo, G.C.F. Chan, Biomaterials **28**, 4652 (2007). doi:10.1016/j.biomaterials.2007.07.041
18. K. Bailey, F.R. Bettelheim, L. Lorand, W.R. Middlebrook, Nature **167**, 233 (1951). doi:10.1038/167233a0
19. F.H. Silver, M.C. Wang, G.D. Pins, Biomaterials **16**, 891 (1995). doi:10.1016/0142-9612(95)93113-R
20. P. Schneider, T. Foitzik, U. Pohlen, W. Golder, H.J. Buhr, J. Surg. Res. **107**, 186 (2002). doi:10.1006/jsre.2002.6511
21. L. Muszbek, V.C. Yee, Z. Hevessy, Thromb. Res. **94**, 271 (1999). doi:10.1016/S0049-3848(99)00023-7
22. J.C. Schense, J.A. Hubbell, Bioconjug. Chem. **10**, 75 (1999). doi:10.1021/bc9800769
23. E.D. Grassl, T.R. Oegema, R.T. Tranquillo, J. Biomed. Mater. Res. **60**, 607 (2002). doi:10.1002/jbm.10107
24. M.R. Neidert, E.S. Lee, T.R. Oegema, R.T. Tranquillo, Biomaterials **23**, 3717 (2002). doi:10.1016/S0142-9612(02)00106-0
25. J.L. Long, R.T. Tranquillo, Matrix Biol. **22**, 339 (2003). doi:10.1016/S0945-053X(03)00052-0
26. D.A. Gabriel, K. Muga, E.M. Boothroyd, J. Biol. Chem. **267**, 24259 (1992)
27. J.P. Collet, J. Soria, M. Mirshahi, M. Hirsch, F.B. Dagonnet, J. Caen et al., Blood **82**, 2462 (1993)
28. S. Cox, M. Cole, B. Tawil, Tissue Eng. **10**, 942 (2000). doi:10.1089/1076327041348392
29. P.S. Ciano, R.B. Colvin, A.M. Dvorak, J. McDonagh, H.F. Dvorak, Lab. Invest. **54**, 62 (1986)
30. D. Eyrich, F. Brandl, B. Appel, H. Wiese, G. Maier, M. Wenzel et al., Biomaterials **28**, 55 (2007). doi:10.1016/j.biomaterials.2006.08.027
31. A. Hokugo, T. Takamoto, Y. Tabata, Biomaterials **27**, 61 (2006). doi:10.1016/j.biomaterials.2005.05.030
32. Y.H. Gong, L.J. He, Z.W. Ma, Q.L. Zhou, Z.W. Ma, C.Y. Gao et al., J. Biomed. Mater. Res. Part B **82B**, 192 (2007)
33. A. Schindler, D. Harper, J. Polym. Sci. A-Polym. Chem (Kyoto) **17**, 2593 (1979)
34. A. Dresdale, E.A. Rose, V. Jeevanandam, K. Reemtsma, F.O. Bowman, J.R. Malm, Surgery **97**, 750 (1985)
35. H.G. Zhao, L. Ma, J. Zhou, Z.W. Mao, C.Y. Gao, J.C. Shen, Biomed Mater. **3**, 015001 (2008). doi:10.1088/1748-6041/3/1/015001
36. Ma ZW, Gao CY, Gong YH, Ji J, Shen JC, J. Biomed. Mater. Res. Part B: Appl. Biomater. **63**, 838 (2002). doi:10.1002/jbm.10470
37. Y.J. Kim, R.L. Sah, J.Y.H. Doong, A.J. Grodzinsky, Anal. Biochem. **174**, 168 (1988). doi:10.1016/0003-2697(88)90532-5
38. R.L.Y. Sah, Y.J. Kim, J.Y.H. Doong, A.J. Grodzinsky, A.H.K. Plaas, J.D. Sandy, J. Orthop. Res. **7**, 619 (1989). doi:10.1002/jor.1100070502
39. C.D. Sims, P.E. Butler, Y.L. Cao, R. Casanova, M.A. Randolph, A. Black et al., Plast. Reconstr. Surg. **101**(6), 1580 (1998). doi:10.1097/00006534-199805000-00022
40. W.J.C.M. Marijnissen, G.J.V.M. Van Osch, J. Aigner, S.W. Van der Veen, A.P. Hollander, H.L. Verwoerd-Verhoef et al., Biomaterials **23**, 1511 (2002). doi:10.1016/S0142-9612(01)00281-2
41. T. Sato, G.P. Chen, T. Ushida, Mater. Sci. Eng. C **17**, 83 (2001). doi:10.1016/S0928-4931(01)00313-7
42. M.S. Rahman, T. Tsuchiya, Tissue Eng. **7**, 78 (2001). doi:10.1089/107632701753337726
43. J.W. Weisel, Adv. Protein Chem. **70**, 247 (2005). doi:10.1016/S0065-3233(05)70008-5
44. E. Malicev, D. Radosavljevic, N.K. Velikonja, Biotechnol. Bioeng. **96**, 364 (2007). doi:10.1002/bit.21038